



Article

Potential of *Suaeda nudiflora* and *Suaeda fruticosa* to Adapt to High Salinity Conditions

Abhishek Joshi¹, Vishnu D. Rajput^{2,*} , Krishan K. Verma³ , Tatiana Minkina² , Karen Ghazaryan⁴ and Jaya Arora^{1,*}

¹ Laboratory of Biomolecular Technology, Department of Botany, Mohanlal Sukhadia University, Udaipur 313001, India

² Academy of Biology and Biotechnology, Southern Federal University, 344090 Rostov-on-Don, Russia

³ Key Laboratory of Sugarcane Biotechnology and Genetic Improvement (Guangxi), Ministry of Agriculture and Rural Affairs/Guangxi Key Laboratory of Sugarcane Genetic improvement/Sugarcane Research Institute, Guangxi Academy of Agricultural Sciences, Nanning 530007, China

⁴ Faculty of Biology, Yerevan State University, Yerevan 0025, Armenia

* Correspondence: rajput.vishnu@gmail.com (V.D.R.); jaya890@gmail.com (J.A.)

Abstract: The deposition of salts in soil seems likely to become a significant barrier for plant development and growth. Halophytes that flourish in naturally saline habitats may sustain extreme salt levels by adopting different acclimatory traits. Insight into such acclimatory features can be useful for devising salt-resilient crops and the reclamation of saline soil. Therefore, salinity-induced responses were studied in two halophytes, i.e., *Suaeda nudiflora* and *Suaeda fruticosa*, at a high soil salinity level (ECe 65) to explore their possible tolerance mechanisms in their natural habitat. Samples of different tissues were collected from both *Suaeda* species for the determination of physio-biochemical attributes, i.e., ionic (Na^+ , K^+ , Ca^{2+} , Cl^-) content, osmo-protective compounds (proline, soluble sugars, soluble proteins), total phenolic content, and antioxidant components. Heavy metal composition and accumulation in soil and plant samples were also assessed, respectively. Fourier transform infrared spectroscopy (FTIR) analysis was conducted to explore cellular metabolite pools with respect to high salinity. The results showed that both species considerably adjusted the above-mentioned physio-biochemical attributes to resist high salinity, demonstrated by quantitative differences in their above-ground tissues. The FTIR profiles confirmed the plants' differential responses in terms of variability in lipids, proteins, carbohydrates, and cell wall constituents. The high capacity for Na^+ and Cl^- accumulation and considerable bioaccumulation factor (BAF) values for metals, mainly Fe and Zn, validate the importance of both *Suaeda* species as phytodesalination plants and their potential use in the phytoremediation of salt- and metal-polluted soils.

Keywords: antioxidants; adaptive mechanism; halophytes; phytoremediation; soil salinity



Citation: Joshi, A.; Rajput, V.D.; Verma, K.K.; Minkina, T.; Ghazaryan, K.; Arora, J. Potential of *Suaeda nudiflora* and *Suaeda fruticosa* to Adapt to High Salinity Conditions. *Horticulturae* **2023**, *9*, 74. <https://doi.org/10.3390/horticulturae9010074>

Academic Editors: Adalberto Benavides-Mendoza, Yolanda González-García, Fabián Pérez Labrada and Susana González-Morales

Received: 5 December 2022

Revised: 29 December 2022

Accepted: 4 January 2023

Published: 6 January 2023



Copyright: © 2023 by the authors. Licensee MDPI, Basel, Switzerland. This article is an open access article distributed under the terms and conditions of the Creative Commons Attribution (CC BY) license (<https://creativecommons.org/licenses/by/4.0/>).

1. Introduction

Soil or land salinization is a severe ecological problem worldwide that consistently increases nearly 10% annually. Nowadays, more than 3% (424 mha) of global topsoil (0–30 cm) and more than 6% (833 mha) of global sub-soil (30–100 cm) are affected by salinity or sodicity. Remarkably, more than two-thirds of global salt-contaminated soils are established in arid and semi-arid climatic zones, of which 64% are located in arid deserts and steppes [1]. Individually, Europe has a maximum share of saline land, which accounts for nearly 3.3% of the world's total saline land. In the rest of the world, including Asia, Africa, America, and Australia, the majority of cultivated land has been salinized and become uncultivable [2]. Salt accumulation in the soil constrains agricultural production and the global economy. It has been estimated that the per hectare cost of salinity-induced land degradation is approximately USD 441, which is further responsible for the loss of USD 27 billion per annum [3]. In India, soil salinization is highly worrisome in arid and

semi-arid areas as it obstructs plant growth and can ultimately limit the distribution of plant communities [4,5].

Salinity imposes deleterious impacts on plants' basic physiology and metabolism in the form of ionic toxicity and osmotic and oxidative stress [6]. Halophytes are plants that grow throughout salty environments and are able to not only sustain but also proliferate by implementing distinct adaptive mechanisms, such as (a) accumulation, exclusion, or compartmentalization of toxic ions at the cellular or whole-plant level, (b) synthesis and accumulation of osmo-protective compounds, i.e., proline, glycine betaine, etc., (c) activation of enzymatic and non-enzymatic antioxidant activities, and (d) modulation of various metabolic cascades, such as the photosynthetic pathway, plant hormones, and signaling molecules [7–9]. In addition, salinity tolerance varies among species of taxonomically identical or related taxa, which should be attributed to plant habitat, growth form, and some specialized structures such as the salt gland, salt bladder, and Kranz anatomy [10,11]. Several studies have reported that halophytes of the same habitat, even the same taxa, respond differently to salinity levels through quantitative and qualitative differences in their response mechanisms [12–14].

The present study explored two species of *Suaeda* (Figure 1), namely *Suaeda nudiflora* (Willd.) Moq., and *Suaeda fruticosa* (L.) Forssk., that dominate a hypersaline region close to the Thar Desert. Despite being genetically identical, these species differ slightly in their aerial morphology, which has been reported as an adaptation to saline conditions [15]. *Suaeda nudiflora* is a perennial under-shrub with smooth stems, elliptic-oblong or linear-obovate glabrous leaves, like spike inflorescences, and black seeds with curved embryos. *Suaeda fruticosa* is a perennial shrub with an erect glabrous stem, usually about 3 m tall, with fleshy and subsessile oblong or elliptic leaves and black seeds. They are considered cash crops because of their medicinal, nutritional, and economic value, as well as their potential use in phytoremediation [16–18].



(a)

(b)

Figure 1. Appearance of the plants in their native environment, (a) = *Suaeda nudiflora*, (b) = *Suaeda fruticosa*.

Several investigations have described salinity-induced modulations, particularly in *Suaeda* species [19,20]. A few studies have examined these two species under controlled laboratory conditions [21–23]. However, there is scant information about their responses in habitats with high salt exposure and which acclimatory mechanisms help the plants complete their life cycle under high salinity circumstances. Studies on the differential behavior of halophytes in their natural habitats can help explain species-specific salt tolerance and provide a framework for the development of salt-resilient crops and a restoration strategy for saline soils [24–26].

The current study aimed to assess the influence of soil salinity on the differential physiological traits of both *Suaeda* species. The hypothesis expressed here is that the successful adaptation of different *Suaeda* species to high salinity conditions is determined by both the magnitude of salinity in their rhizosphere soil as well as their individual salt tolerance evolutionary strategies. Furthermore, species-specific and common physiological responses may operate within the species. In order to gain insight into possible common and species-specific tolerance mechanisms in these species, a comparative study of their physiological responses to the physicochemical attributes of rhizospheric soil would be a useful approach. This study is designed specifically to (i) identify key biochemical indicators and cellular metabolites of *Suaeda nudiflora* and *Suaeda fruticosa* relevant to their tolerance mechanism towards high salinity, and (ii) determine the bioaccumulation capacity of salts and heavy metals by both species for phytoremediation purposes in the future.

2. Materials and Methods

2.1. Description of Sampling Site

The sampling site, Sambhar Salt Lake (26°58'0" N to 75°5'0" E), which is recognized as India's largest inland salt lake, was chosen to represent high soil salinity levels. The lake is elliptically shaped, with a length of approximately 36 km, a breadth varying 3–11 km, and located in the Rajasthan state of India (Figure 2). It is an extensive saline wetland, receiving water from six rivers, including the Medtha, Samaod, Mantha, Rupangarh, Khari, and Khandela. The eastern area of the lake is accompanied by numerous salt reservoirs, canals, salt pans, and halophyte vegetation [27]. It is estimated that silt from the Aravalli hills, which is generally encrusted in schists (medium-grade metamorphic rock) and gneisses (high grade regional metamorphic rock), is the major source of the salt composites. The sodium composites in the silt dissolve in rainwater and enter the lake via rivers, and the salt remains in the lake after the rainwater evaporates [28]. Extremely hot summers and mild winters are features of the temperate-continental environment. The average annual temperature was 25.1 °C with a multiannual minimum of 5 °C and maximum of 50 °C in May/June.

2.2. Collection and Analysis of the Samples

In the month of May 2019, soil and plant samples (sampled area; 10 m × 15 m, sample weight; 100 g) were collected in order to ascertain the physicochemical properties. The soil samples were drawn from a depth of 20–25 cm, carefully packed inside polybags, and sent to the laboratory for further examination and analysis. The experiments were performed in triplicate. At the same location, 12 plants of each species were carefully taken out of the soil and maintained at 4 °C to prevent the destruction of the sample's constituents until analysis.

2.3. Soil Analysis

Standardized protocols described in the USDA Handbook were applied to calculate the pH, electric conductivity (ECe), and organic carbon (OC) content of the soil [29]. The accessibility of phosphorous (available form P₂O₅) and potassium content (available form K₂O) were determined by the methods described by Olsen [30] and Merwin and Peech [31], respectively. According to the method described by Prakash and Prathapasenan [32], the soluble salt content was determined after extraction with distilled water (soil: water ratio,

1:5) using a flame photometer (Eppendorf; Na^+ and K^+), atomic absorption spectrometer (Perkin Elmer, Analyst 200, Rodgau, Germany; Ca^{2+}), and chloridometer (Buchler-Cotlove; Cl). With the use of an atomic absorption spectrometer (Perkin Elmer, Analyst 200 Germany), the availability of iron (Fe), zinc (Zn), manganese (Mn), and copper (Cu) was assessed following digestion with a di-acid mixture (HCl/HNO_3 mixture and concentrated HClO_4) according to Tüzen's technique [33].

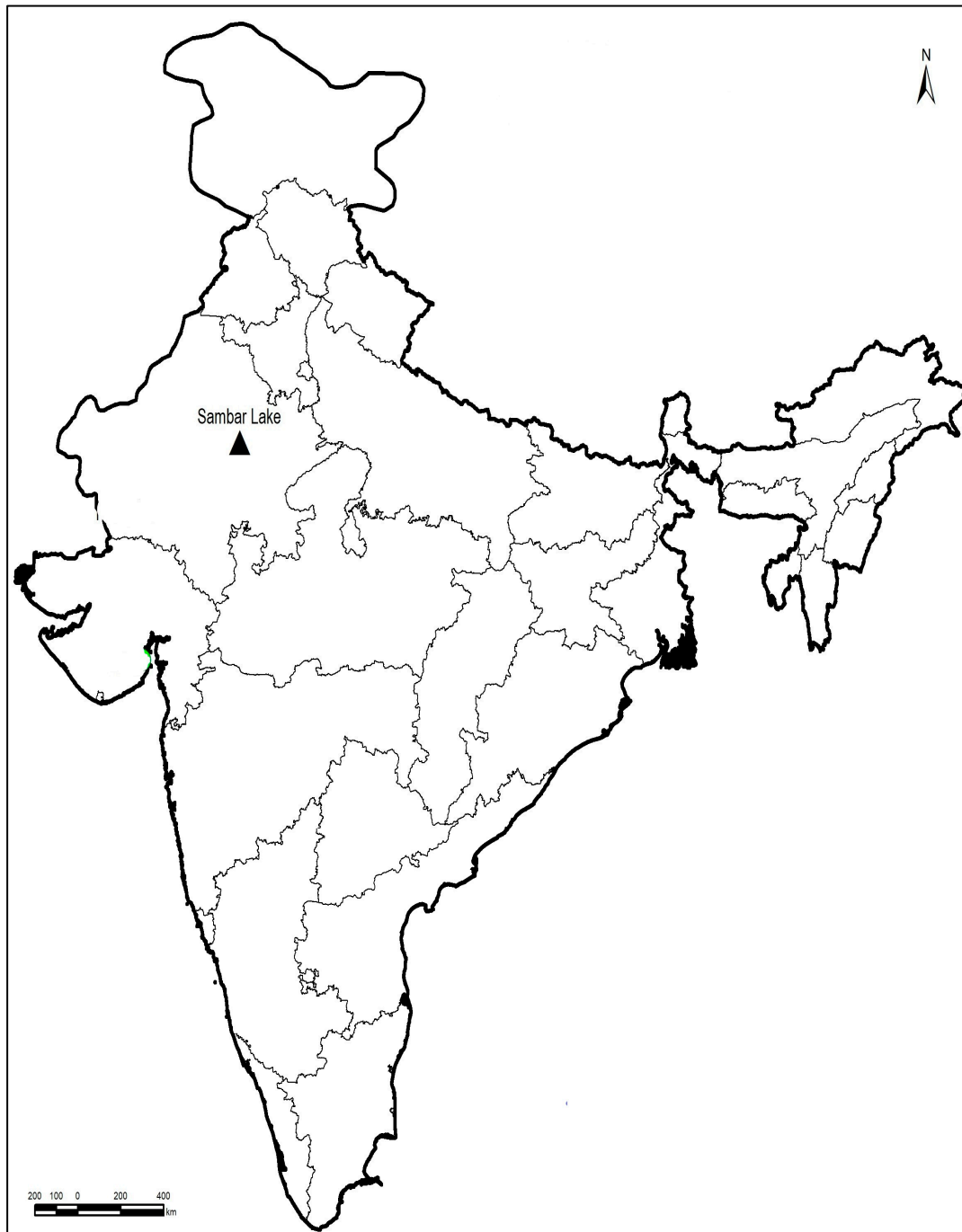


Figure 2. GIS map of the sampling site.

2.4. Determination of Soluble Ions in Plants

Plant parts such as the leaves and stem were cleaned and dried inside an oven at $60\text{ }^\circ\text{C}$ for 72 h. The completely dried leaves and stem were ground into a fine powder using a mortar and pestle. The extracts were prepared by digestion with HNO_3 , according

to Prakash and Prathapasenan [32]. Similar to the soil above, the concentrations of Na^+ , K^+ , Ca^{2+} , and Cl^- in the plant extract were determined using a flame photometer, atomic absorption spectrometer, and chloridometer, respectively.

2.5. Determination of Osmo-Protective Compounds

The ninhydrin technique was utilized to quantify the proline content [34]. Soluble proteins were assessed according to the Bradford method [35] using bovine serum albumin as the standard. A modification of the phenol–sulfuric acid method was used to determine the total soluble sugar content [36].

2.6. Determination of Total Phenolic Content (TPC) and Antioxidant Activity

A 250 mg sample of dried powdered plant material was extracted with 5 mL of 70% methanol and dried in test tube rotator at room temperature for 12 h. The total phenolic content (TPC) and antioxidant activity of the extract were determined in triplicate. Phenolic compound analysis was performed using Foline-Ciocalteu reagent with the Farkas and Kiraly method [37]. TPC was calculated using a calibration curve for gallic acid at 650 nm and represented as mg gallic acid equivalents (GAE g^{-1} DW). The method described by Hatano et al. [38] was used to measure the 1,1-diphenyl-2-picrylhydrazyl (DPPH) radical scavenging activity. DPPH scavenging activity (%) was calculated as $(\%) = 100(A - B)/A$, where A and B are the control and corrected absorption of the sample reaction mixture at 517 nm, respectively. The Benzie and Strain technique [39] was applied to calculate the ferric reducing power (FRAP).

2.7. Determination of Metal Contents and Bioaccumulation Factor in Plants

After separating the plant parts (leaves and stem), they were completely cleaned with distilled water and then dried in an oven at 65 °C. The dried plant organs (0.5 g) were heated in a muffle furnace at 550 °C for 12 h. Subsequently, an extract was made in accordance with the method described by Tuzen [33], and an atomic absorption spectrometer was employed to measure the amount of metals in the plant sample extract (Perkin Elmer, Analyst 200 Germany). The ratio of the concentrations of metal in various parts of the plant is known as the bioaccumulation factor (BAF). BAF refers to the ability of plants to take up, transport, and store metals in its above-ground tissue [40], and it was determined as follows:

(BAF) Leaves: $[\text{Metal in leaves tissue}]/[\text{Metal in soils}]$

(BAF) Stem: $[\text{Metal in stem tissue}]/[\text{Metal in soils}]$

2.8. Fourier Transform Infrared Spectroscopy (FTIR) Analysis

FTIR analysis was used to identify functional groups in the leaves and stem parts of the plants. Three different samples of leaves and stem were taken from both species for FTIR analysis. Thereafter, pelleted samples of leaves and stem were scanned in the mid-infrared region ($4000\text{--}400\text{ cm}^{-1}$) using an FTIR spectrometer (Bruker, Model OPUS 7.5.18). These samples contributed to the generation of three unique FTIR spectra. Analysis software was used for the identification of functional groups in the leaves and stem samples.

2.9. Experimental Design and Statistical Analysis

The study was carried out using a complete randomized block design (CRBD), which was performed twice. In every test, soil and plant samples were replicated at least three times ($n = 3$). Duncan's multiple range test as used to determine whether there was a statistically significant difference ($p < 0.05$) between the means of the different species. The results are presented as the mean \pm SD of three separate trials, which were then analyzed using one-way analysis of variance (ANOVA). Statistical analysis was performed using SPSS version 17 software (SPSS Inc., Chicago, IL, USA).

3. Results

3.1. Soil Physicochemical Properties

The physicochemical properties of the soil at the sampling sites are summarized in Table 1. The soil in the study area had an alkaline nature with high values for pH (9.89) and ECe (65 dS/m⁻¹). The average available organic carbon content and phosphorous and potassium concentrations were 0.19%, 8.49 kg/ha, and 84.13 kg/ha, respectively. Among the soluble cations, the concentration of Na⁺ was relatively high (1485 mg/100 g) followed by K⁺ (41.23 mg/100 g) and Ca²⁺ (19.51 mg/100 g). The average Cl⁻ concentration was 1.02 mg/100 g. Heavy metal analysis of the soil sample revealed Fe as the major metal ion with the highest concentration (4185 mg/kg), followed by Zn (38.64 mg/kg), Mn (131.9 mg/kg), and Cu (6.47 mg/kg).

Table 1. Physicochemical properties of the soil at the collection sites (mean ± SD, n = 3).

S. No.	Parameters	Values
1	Soil pH	9.89 ± 0.6
2	ECe (dS/m ⁻¹)	65 ± 0.7
3	Organic carbon (%)	0.19 ± 0.04
4	P ₂ O ₅ (kg/ha)	8.49 ± 0.32
5	K ₂ O (kg/ha)	84.13 ± 0.79
6	Na ⁺ (mg/100 g dry soil)	1485 ± 16.11
7	K ⁺ (mg/100 g dry soil)	41.23 ± 2.4
8	Ca ²⁺ (mg/100 g dry soil)	19.51 ± 1.8
9	Cl ⁻ (mg/100 g dry soil)	1.02 ± 0.74
10	Iron (mg/kg)	4185 ± 70.4
11	Zinc (mg/kg)	38.64 ± 1.85
12	Manganese (mg/kg)	131.9 ± 4.6
13	Copper (mg/kg)	6.47 ± 0.97

3.2. Accumulation of Soluble Ions in Plants

The amount of solubilized ions in the different tissues of both species was affected by the salinity, as indicated in Table 2. Measurement of cation (Na⁺, K⁺, Ca²⁺) and anion (Cl⁻) concentrations in the plants revealed clear differences between the species, with relatively high concentrations in *S. fruticosa*. The corresponding value was higher in the leaves than in the stem and was higher in *S. fruticosa* leaves. Except for Ca²⁺, the mean concentrations of soluble ions were approximately 1.5-fold higher in the *S. fruticosa* leaves (Na⁺ 71.01 mg/g; K⁺ 19.54 mg/g; Cl⁻ 14.02 mg/g) than in the *S. nudiflora* leaves (Na⁺ 45.56 mg/g; K⁺ 12.65 mg/g; Cl⁻ 11.68 mg/g).

Table 2. Deposition of various ions in leaves and stem parts of the plants.

Species	Plant Parts	Na ⁺	K ⁺	Ca ²⁺	Cl ⁻	Na ⁺ /K ⁺ Ratio
<i>S. nudiflora</i>	Leaves	45.56 ± 1.34 ^b	12.65 ± 1.05 ^b	11.72 ± 1.12 ^b	11.68 ± 1.21 ^b	3.60
	Stem	21.32 ± 1.08 ^d	7.63 ± 0.98 ^d	6.89 ± 0.65 ^d	5.56 ± 0.99 ^d	2.79
<i>S. fruticosa</i>	Leaves	71.01 ± 1.71 ^a	19.54 ± 1.45 ^a	11.54 ± 0.91 ^a	14.02 ± 1.01 ^a	3.63
	Stem	23.84 ± 1.19 ^c	8.55 ± 0.77 ^c	7.90 ± 0.84 ^c	7.11 ± 1.18 ^c	2.78

Note: Statistically significant differences ($p \leq 0.05$) between plant parts are marked with superscripts a, b, c, and d.

In the stem, the concentrations of soluble ions were approximately 1.2-fold higher in *S. fruticosa* (Na⁺ 23.84 mg/g; K⁺ 8.55 mg/g; Ca²⁺ 7.90 mg/g; Cl⁻ 7.11 mg/g) than in *S. nudiflora* (Na⁺ 21.32 mg/g; K⁺ 7.63 mg/g; Ca²⁺ 6.89 mg/g; Cl⁻ 5.56 mg/g). Given the Na⁺ and K⁺ accumulation patterns in the different tissue, the Na⁺/K⁺ ratio was relatively high in the leaves (3.6 on average) compared to that in the stem tissue (2.8) of both species.

3.3. Accumulation of Osmo-Protective Compounds

Measurements of common osmo-protective compounds in plants, including proline, total soluble sugar (TSS), and total soluble proteins (TSP), are presented in Table 3. Proline and TSS were probably the dominant osmo-protective compounds in both species. The absolute concentrations of accumulated proline in the stem were significantly greater than in the leaves, by nearly 2-fold, and were highest in the *S. nudiflora* stem (22.41 μ moles/g). The corresponding values of TSS were higher in the leaves than in the stem, with minor quantitative differences between species.

Table 3. Deposition of osmo-protective chemicals in leaves and stem parts of halophytes.

Species	Plant Part	Proline Content (μ moles/g)	Soluble Sugar Content (mg/g)	Soluble Protein Content (mg/g)
<i>S. nudiflora</i>	Leaves	7.99 \pm 0.20 ^d	9.87 \pm 0.36 ^a	7.23 \pm 0.91 ^a
	Stem	22.41 \pm 0.30 ^a	6.35 \pm 0.38 ^b	3.24 \pm 0.13 ^c
<i>S. fruticosa</i>	Leaves	8.82 \pm 0.14 ^c	9.43 \pm 0.24 ^d	4.37 \pm 0.41 ^b
	Stem	18.57 \pm 0.90 ^b	6.02 \pm 0.26 ^d	1.98 \pm 0.12 ^d

Note: Statistically significant differences ($p \leq 0.05$) between plant parts are marked with superscripts a, b, c, and d.

The highest value of TSS was in the *S. nudiflora* leaves (9.87 mg/g), followed by that in *S. fruticosa* leaves (9.43 mg/g). The absolute concentration of accumulated TSP in the leaves was higher than in the stem, by approximately 2.2-fold, and was highest in the *S. nudiflora* leaves (7.23 mg/g), followed by that in the *S. fruticosa* leaves (4.37 mg/g).

3.4. Estimation of TPC and Antioxidant Activity

The variations in TPC and antioxidant potential of the studied species are illustrated in Figure 3.

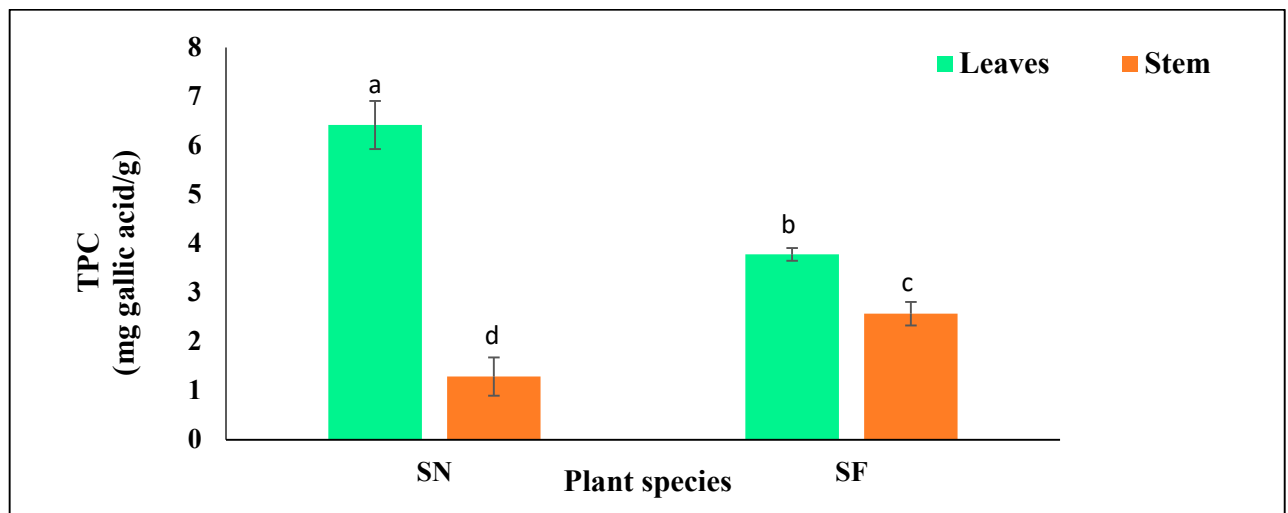
The mean values of TPC were significantly greater in the leaves than in the stem and were 1.7-fold higher in the *S. nudiflora* leaves than in the *S. fruticosa* leaves (Figure 3a). In the case of the stem, its corresponding value was greater in *S. fruticosa* than in *S. nudiflora* by 2-fold.

Remarkably, both species displayed differential trends to scavenge the free ferric and DPPH radical ions. In *S. nudiflora*, the free ferric radical ion scavenging potential was significantly greater in the leaves than in the stem, while in *S. fruticosa*, it was greater in the stem than in the leaves, by 1.7- and 1.45-fold, respectively (Figure 3b). Similarly, the DPPH radical scavenging potential was significantly greater in the leaves of *S. nudiflora*, while it was greater in the stem in the case of *S. fruticosa* by 1.03-fold (Figure 3c).

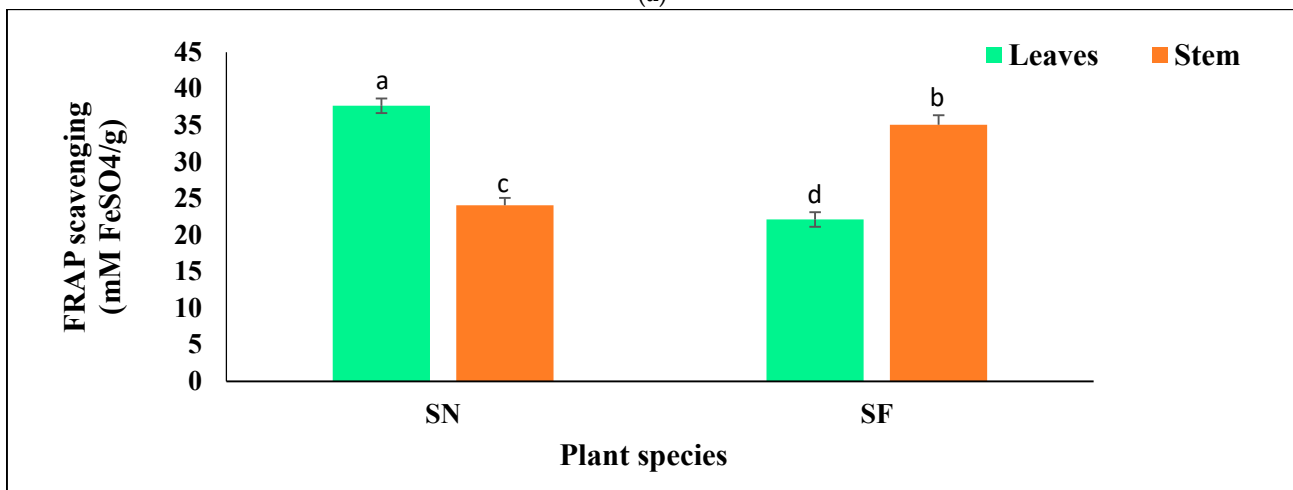
3.5. Estimation of Metal Concentrations in Leaves and Stem Parts of Plants

The concentrations of several metals, such as Zn, Mn, Fe and Cu, in the leaves and stem parts of the two species of plant with similar habitat are shown in Figure 4. The metal analysis of the plants revealed Fe as the major metal ion, followed by Zn, Mn, and Cu.

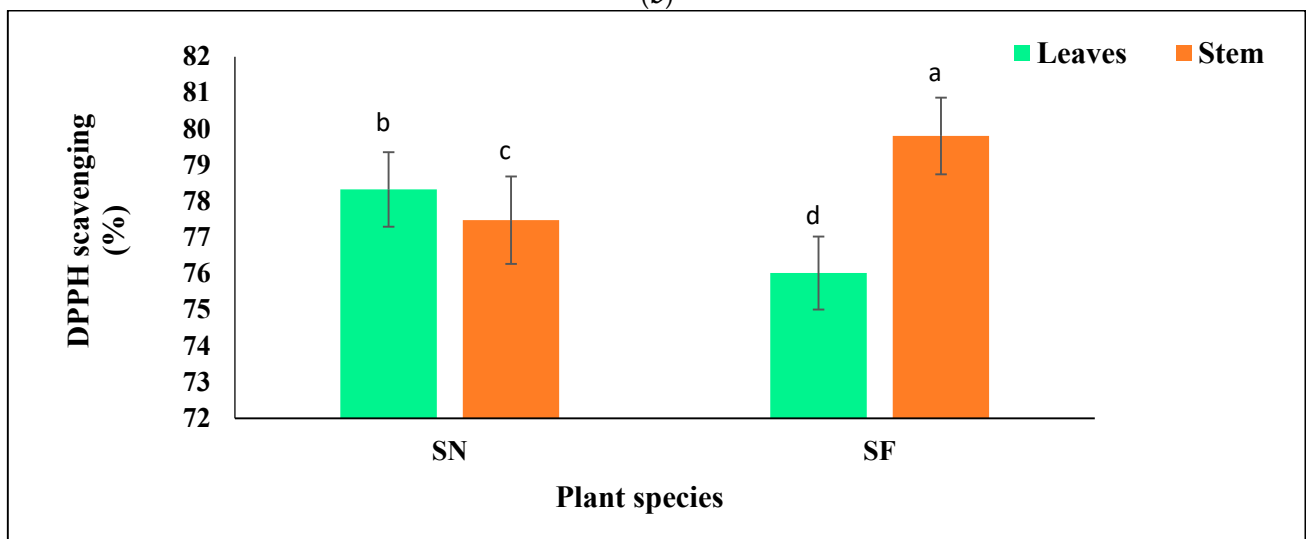
The mean Fe concentration ranged from 59.91 to 61.37 mg/kg and was highest in the *S. nudiflora* leaves. Nevertheless, its corresponding BAF value was similar in both species and remained very low (0.014). The Zn concentration ranged from 15.61 to 17.59 mg/kg and was highest in the *S. nudiflora* stem. The bioaccumulation factor (BAF) values for Zn ranged from 0.403 to 0.455 and were highest in the *S. nudiflora* stem (Table 4). The mean Mn concentration varied from 11.23 to 12.22 mg/kg and was highest in the *S. fruticosa* leaves. The BAF value for Mn was low, ranging from 0.085 to 0.094. Similarly, the mean Cu concentration varied from 2.13 to 2.89 mg/kg and was highest in the *S. fruticosa* leaves. The corresponding BAF value for Cu ranged from 0.329 to 0.446 and was highest in the *S. fruticosa* leaves.



(a)



(b)



(c)

Figure 3. TPC and antioxidant (FRAP and DPPH) activity in leaves and stem parts of the plants (DMRT), (a) = TPC, (b) = FRAP, (c) = DPPH, SN = *S. nudiflora*, SF = *S. fruticosa*. Note: Statistically significant differences ($p \leq 0.05$) between plant parts are marked with superscripts a, b, c, and d.

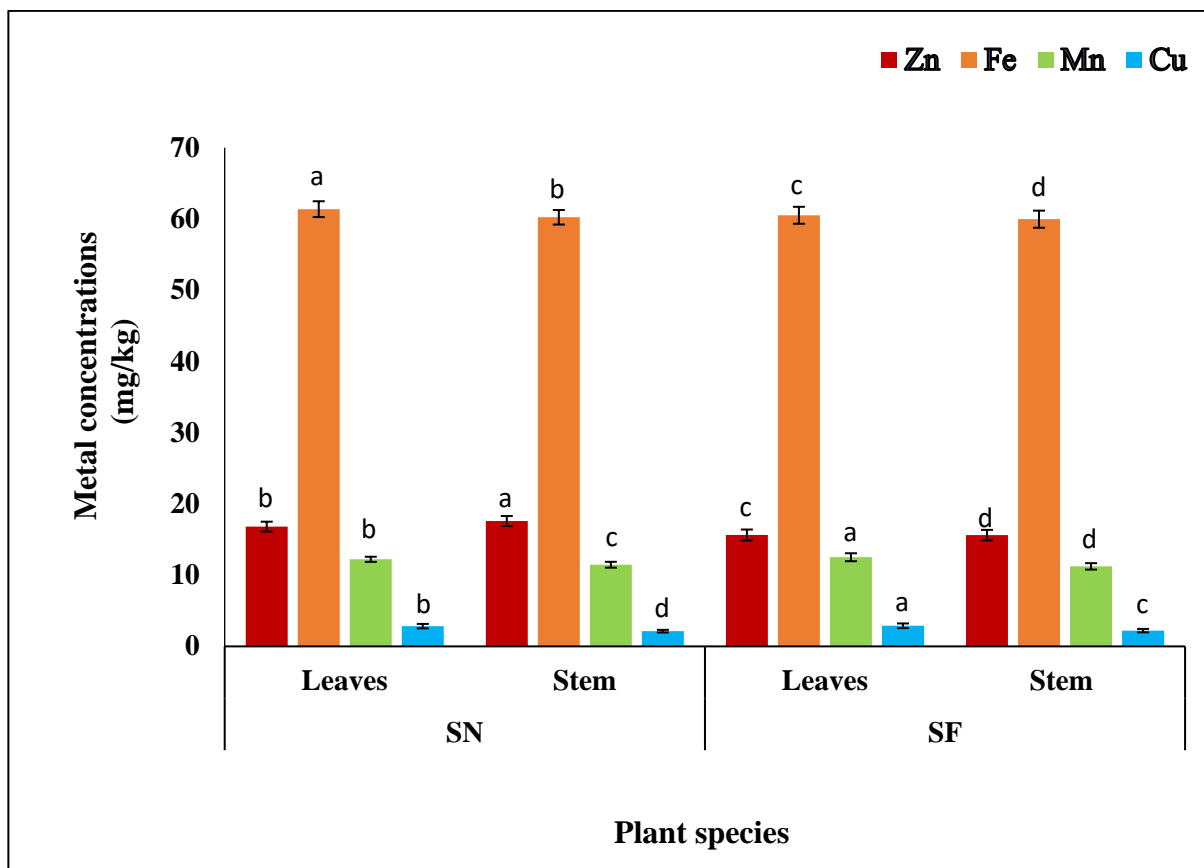


Figure 4. Concentrations of various metal ions in leaves and stem parts of the plants (DMRT), SN = *S. nudiflora*, SF = *S. fruticosa*. Note: Statistically significant differences ($p \leq 0.05$) between plant parts are marked with superscripts a, b, c, and d.

Table 4. Bioaccumulation factor (BAF) values for metals in leaves and stem of plants species.

Species	Plant Parts	Metals			
		Zn	Fe	Mn	Cu
<i>S. nudiflora</i>	Leaves	0.435 ± 0.17	0.014 ± 0.01	0.092 ± 0.05	0.438 ± 0.21
	Stem	0.455 ± 0.23	0.014 ± 0.01	0.086 ± 0.03	0.329 ± 0.14
<i>S. fruticosa</i>	Leaves	0.404 ± 0.15	0.014 ± 0.01	0.094 ± 0.07	0.446 ± 0.20
	Stem	0.403 ± 0.11	0.014 ± 0.01	0.085 ± 0.03	0.341 ± 0.16

Note: Data are presented as the mean ± SD of three separate trials.

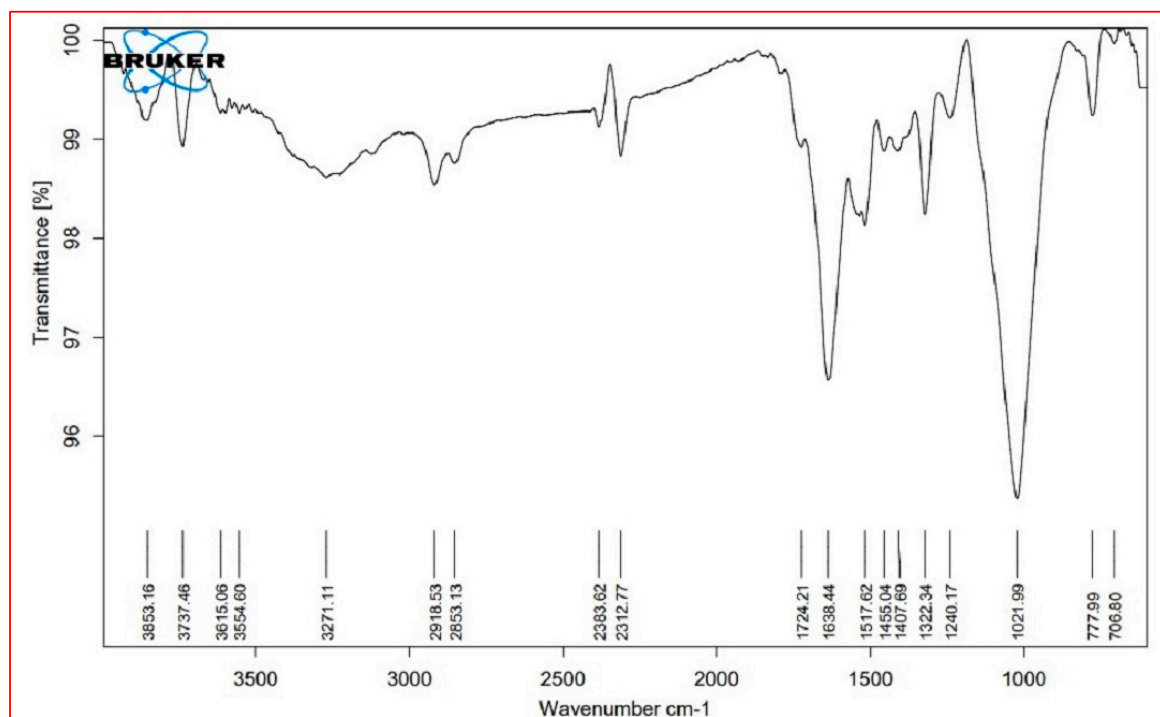
3.6. FTIR Analysis

The major FTIR spectra peaks and possible functional groups present in the leaves and stem parts of both plant species are shown in Table 5 and Figure 5. The wavenumber region 3000–2000 cm^{-1} was assigned to lipids. In this region, both species showed a similar FTIR profile, except for a peak at 2921 cm^{-1} , which was not present in the leaves of *S. nudiflora* (Figure 5a). This peak indicated the presence of O–H stretch (Alcohols), S, O–H stretch (carboxylic acids), and =C–H (benzene, alkynes, alkenes). Additionally, the peak at 2854 cm^{-1} was not present in the stem of both species (Figure 5b,d). This peak indicated the presence of C–H stretch (alkenes) and H–C=O:C–H stretch (aldehydes).

Table 5. FTIR spectra illustrating various peaks of functional groups in leaves and stem parts of the plants.

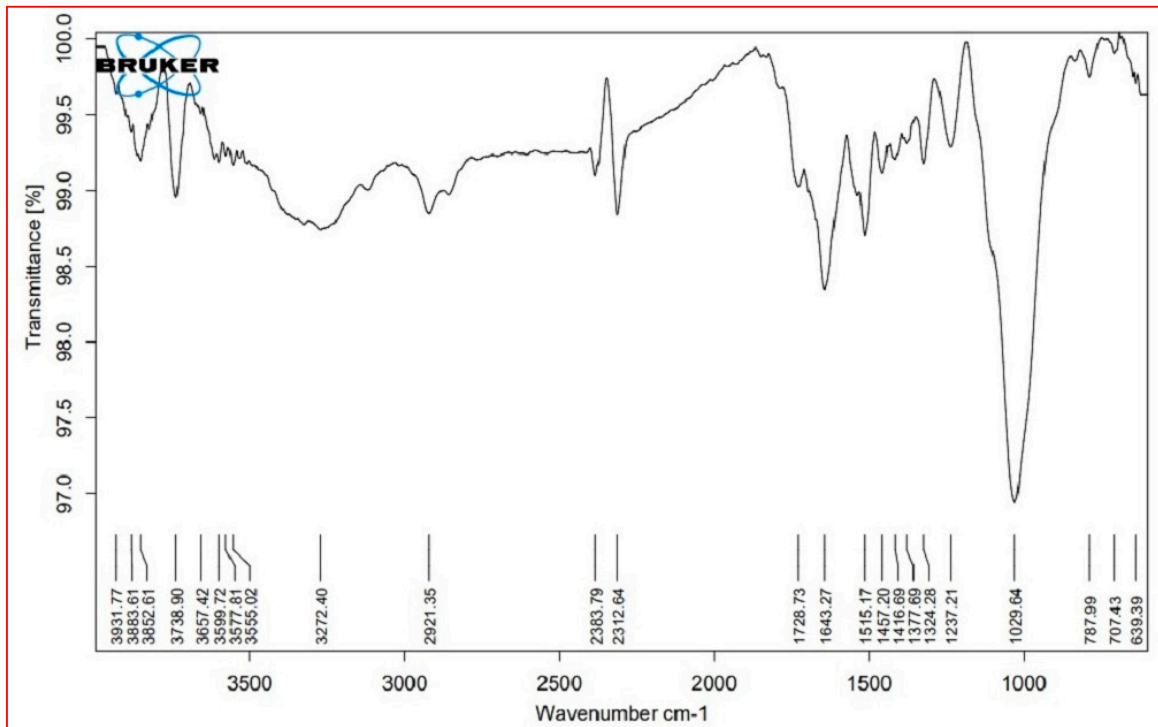
Cellular Metabolites	Wavenumber (cm ⁻¹)				Probable Functional Group
	<i>S. nudiflora</i>		<i>S. fruticosa</i>		
	Leaves	Stem	Leaves	Stem	
Lipids (3000–2000 cm ⁻¹)	3853.16 ±0.94	3825.61 ±0.91	3853.00 ±1.02	3852.86 ±0.98	O–H stretch (alcohols, phenols)
	3737.46 ±0.72	3738.90 ±0.51	3737.97 ±0.64	3739.05 ±0.85	O–H stretch (alcohols)
	*	2921.35 ±0.63	2921.95 ±0.41	2923.88 ±0.33	O–H stretch (alcohols), S, O–H stretch (carboxylic acids), =C–H (benzene, alkynes, alkenes)
	2853.13 ±0.55	*	2854.78 ±0.61	*	C–H stretch (alkenes), H–C=O:C–H stretch (aldehydes)
	2383.62 ±0.52	2383.79 ±0.49	2384.10 ±0.52	2383.87 ±0.37	P–H (phosphine)
	2312.77 ±0.43	2312.64 ±0.64	2312.28 ±0.50	2312.42 ±0.73	C=C stretch (alkynes)
	Proteins (1800–1500 cm ⁻¹)	1724.21 ±0.39	1728.73 ±0.42	*	*
1638.44 ±0.13		1643.27 ±0.28	1641.08 ±0.21	1642.24 ±0.26	N–H bend (nitro compounds, amides), C–C stretch (amides), C=O stretch (carboxylic acid, ketone), C=C (benzene, alkenes)
1517.62 ±0.18		1515.17 ±0.25	1517.66 ±0.10	1514.58 ±0.14	N–H bend (nitro compounds), C–O stretch (amides), C=C (benzenes), C=O (ketones)
1455.04 ±0.16		1457.20 ±0.23	1460.25 ±0.24	1457.18 ±0.20	C–C stretch (aromatics), C–H bend (alkanes), N–O stretch (nitro compounds), C–O stretch (esters), CO–H bend (aldehydes), O–H bend (alcohols)
Carbohydrates (1500– 1000 cm ⁻¹)	*	1377.69 ±0.57	*	1377.27 ±0.13	N=O, CO–H band, O–H band
	1322.34 ±0.27	1322.34	±0.27	1323.60 ±0.63	S(=O) ₂ stretch (sulfoxides), N=O stretch (nitro compounds), O–H bend (carboxylic acids, alcohols)
	1240.17 ±0.31	1237.21 ±0.29	1237.34 ±0.25	1233.55 ±0.54	C–N stretch (amines), C–O stretch (esters), C–O stretch (ethers, alcohols), O–H band (carboxylic acids)
	1021.99 ±0.18	1029.64 ±0.23	1030.39 ±0.12	1030.27 ±0.20	S=O stretch (sulfoxides), C–N stretch (amines), C–O stretch (esters, ethers, alcohols), =C–H bend (benzene, alkenes) (cellulose)
	*	*	818.93 ±0.11	830.21 ±0.16	C–N stretch (amines), =C–H bend (benzene, alkynes) (xyloglucan)
Cell wall components (1000– 600 cm ⁻¹)	777.99 ±0.08	787.99 ±0.15	775.31 ±0.12	782.15 ±0.16	C–N stretch (amines), =C–H bend (benzene), C–C stretch
	*	639.39 ±0.23	*	649.96 ±0.31	C–N stretch (amines), =C–H bend (Benzene), C–C stretch (chloride)

Note: Data are presented as the mean ± SD of three separate trials, * = not determined.

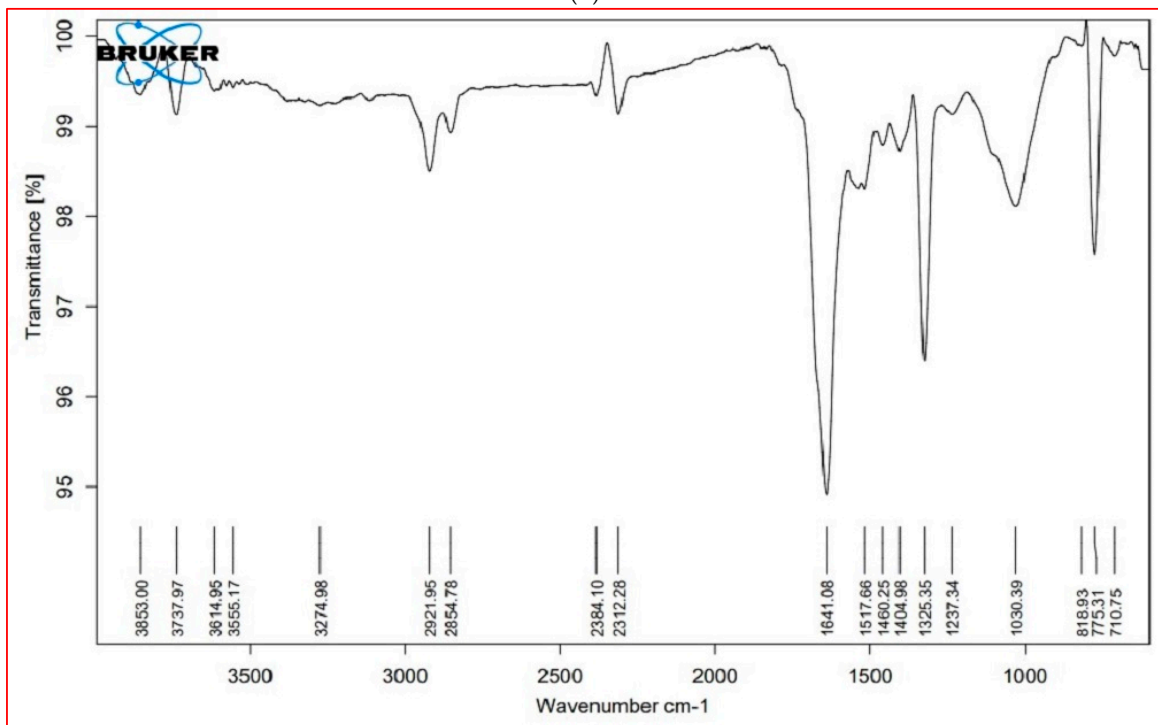


(a)

Figure 5. Cont.



(b)



(c)

Figure 5. Cont.

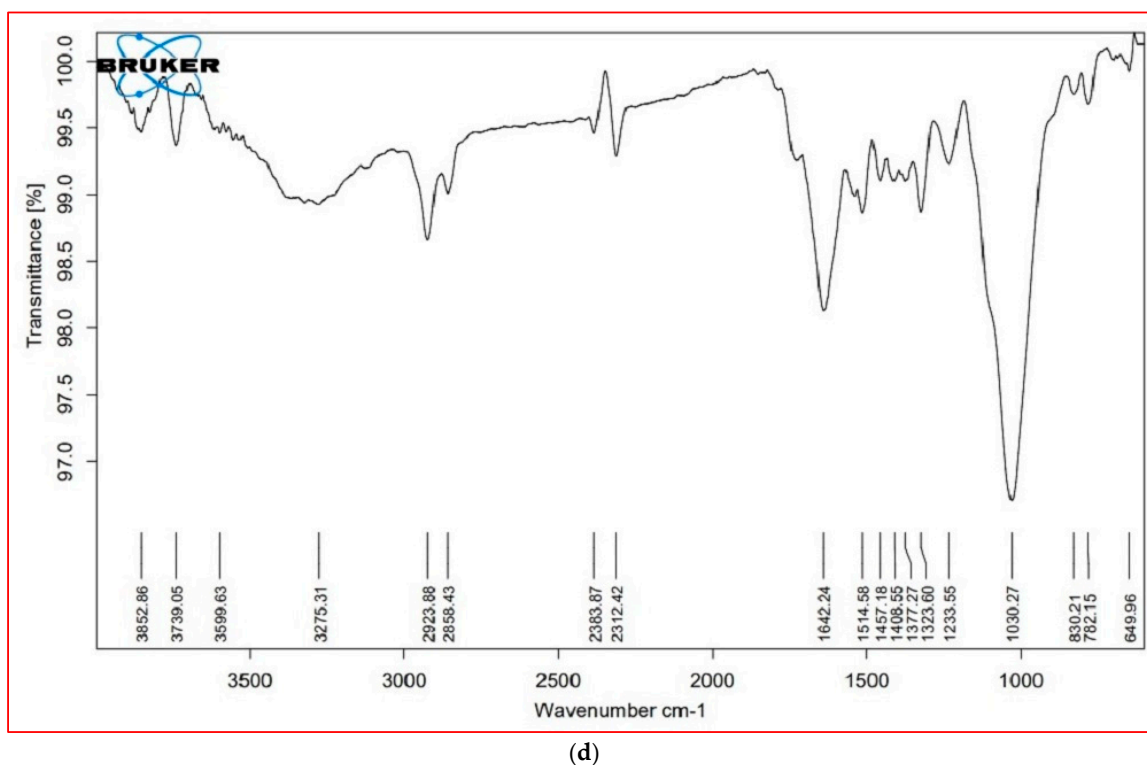


Figure 5. FTIR profiles of different tissue of the plants, (a) = *S. nudiflora* leaves, (b) = *S. nudiflora* stem, (c) = *S. fruticosa* leaves, (d) = *S. fruticosa* stem.

The wavenumber region $1800\text{--}1500\text{ cm}^{-1}$ was assigned to proteins. In this region, both species showed a similar FTIR profile, except for a peak at 1724 cm^{-1} that completely disappeared in *S. fruticosa* (Figure 5c,d). These peaks were characteristic of C=O (esters, carboxylic acids, ketones, aldehydes) and C=C (benzenes). The wavenumber region $1500\text{--}1000\text{ cm}^{-1}$ represented carbohydrates. Except for the peak at 1377 cm^{-1} (characteristic of N=O, CO-H band, and O-H band), both species displayed similar FTIR profiles. The wavenumber region $1000\text{--}600\text{ cm}^{-1}$ was assigned to cell wall components. In both species, a major peak has appeared at 775 cm^{-1} . These peaks were characteristic of C-N stretch (amines), =C-H bend (benzene, alkenes), and C-C (chlorides).

4. Discussion

In arid and semi-arid climates, soil salinization is a vital stress factor that impedes the physiological, biochemical, and molecular attributes of plants and can affect the distribution of plant communities [4,41]. In this study, the sampling site was located near the hyper-arid climate of the Thar Desert, which possesses an alkaline nature with a high ECe value, likely due to the presence of inherent salt sources, a high evaporation rate, and poor surface drainage conditions [15,42]. The ECe value was approximately 17-fold greater than that of cultivated land; therefore, the sampling site could be considered to be a hypersaline habitat. By definition, soil is considered saline when its ECe value is above 4 dS m^{-1} [43]. The higher amount of Na^+ among major cations and Cl^- among anions confirmed the abundance of NaCl salt, which might be responsible for the expansion of hyper salinity at this site. However, its concentration may be subject to seasonal variations due to intricate evaporative mechanisms, particularly during the dry period [28].

pH and ECe values are dominant factors determining the binding and retention capacity of metal ions in soil. They can be used as potential indicators for metal/metalloid pollution [44]. At this site, the corresponding concentrations of metal ions, particularly Fe and Zn, confirmed that metal ions became less mobile and were effectively retained in the soil under high salinity conditions. Although the amounts of all studied metal ions were

within the range of threshold values of Indian standards, their corresponding values may threaten soil fertility and productivity [45].

In this study, a series of acclimatory responses of two halophytes, namely *S. nudiflora* and *S. fruticosa*, were investigated to quantify the impact of high salinity on both species in their natural habitat. It was found that both species adjusted several physio-biochemical attributes to survive in the hypersaline habitat. The results also supported the hypothesis that plants of the same taxa respond differently to salinity levels by means of quantitative and qualitative differences in their response mechanisms [25,26]. Adjustment to ionic toxicity is usually achieved through accumulation or compartmentalization of toxic ions in specific plant cells, tissues, or organs, without affecting plant growth and development [46].

In this study, corresponding concentrations of cations (Na^+ , K^+ , and Ca^{2+}) and anion (Cl^-) were higher in the leaves than in the stem of both species. Additionally, the high Na^+ level was accompanied by elevated levels of K^+ and Ca^{2+} , which might be associated with the conjoint action of anions to confer some degree of halo-tolerance [47]. The facts that K^+ and Ca^{2+} counteract the harmful effects of Na^+ and are essential to sustaining various turgor-driven movements in salt-stressed plants are well clarified and documented [48–50]. A lower Na^+/K^+ ratio in the stem than in the leaves in both species could be part of the constitutive mechanism to maintain ionic homeostasis under high salinity conditions [51]. These findings are consistent with the fact that the internal molecular ratio of Na^+/K^+ in the shoots of dicot halophytes was lower than that of halophyte grasses, indicating some specific features that enabled these dicot species to accumulate, absorb, and compartmentalize Na^+ , thus providing inexpensive osmotic particles for adjusting osmotic pressure [52,53]. Thus, these *Suaeda* species may prove to be beneficial for their possible use in the phytoremediation of saline soils since they accumulate high concentrations of Na^+ and Cl^- ions in comparison with several halophytes that have been previously explored for their potential use in reclaiming saline soil [54–56].

Osmo-protective compounds or osmolytes are well known to accumulate in response to a plant's exposure to abiotic stress conditions [57]. Proline accumulates in the cell as a molecular chaperone, playing a vital role in osmotic stress tolerance by protecting cellular structures and metabolic pools [58]. At the same time, sugars directly contribute to osmotic adjustment and can regulate the expression of stress-responsive genes [59]. In the present study, both species accumulated a significantly high amount of proline in the stem, while accumulating TSS and TSP in the leaves. This finding emphasized that such components are efficient osmoprotectants that help *Suaeda* species tolerate high salinity levels. The high proline level in *Suaeda* species could be associated with the plant's ability to reallocate osmolytes in distinct subcellular compartments in order to compensate for water loss and ionic toxicity [60]. The greater accumulation of TSS in the leaves may be important to stabilize protein structures, thereby increasing protein levels when exposed to salt stress conditions [61,62]. Many halophytes have demonstrated similar osmotic adjustment patterns in salty or alkaline habitats [63,64]. There has been evidence that *Suaeda* species collected from sites with high salinity retain higher amounts of soluble protein, sugars, proline, and total organic osmolytes in their aerial tissues than those collected from low salinity sites [65–67].

Under salinity stress, oxidative damage imposed by reactive oxygen species (ROS) is mitigated through enzymatic and non-enzymatic antioxidants machinery [68]. Among several secondary metabolites, polyphenolic bioactive compounds play crucial roles as hydrogen donors, singlet oxygen quenchers, and reducing agents, which makes them one of the most interesting metabolites of antioxidants [69]. In the present study, the TPC of leaves was significantly higher in comparison to the stem, with 1.7-fold higher levels in the *S. nudiflora* leaves than in the *S. fruticosa* leaves. While in the stem, TPC was 2-fold greater in *S. fruticosa* than *S. nudiflora*. The observed differential accumulation of TPC under salinity stress is an indication that TPC is capable of mitigating the effects of oxidative stress in these species. Moreover, its robust accumulation and synthesis could be dependent on the salt sensitivity of the considered species [70]. Contrary to the accumulation of

phenolic content, both species showed differential trends in order to scavenge the free ferric (Figure 3b) and DPPH radical ions (Figure 3c). In the case of *S. nudiflora*, FRAP and DPPH scavenging activity were significantly higher in the leaves than in the stem, while in *S. fruticosa*, they were much greater in the stem than in the leaves. These results suggest a differential mechanism for FRAP and DPPH scavenging under high salinity conditions in these species. This could be attributed to the fact that halophytes have developed different strategies to avoid cellular oxidative damage by enhancing the phenolic content and other ROS-detoxifying agents combined with enzymatic antioxidants [68,71]. As these plants contain polyphenolic compounds with high antioxidant activities, they should be considered for cultivation in saline soil in order to achieve a sustainable income for farmers living in arid and semi-arid regions.

Salinity can help to improve the mobility of metals/metalloids in plants, mainly because of the structural complexity and antagonistic actions between metal ions and salt-derived anions or cations for sorption sites [72,73]. In the present study, the plant species accumulated Fe as the major metal ion, followed by Zn, Mn, and Cu, while the accumulation patterns significantly differed between species and tissues. This indicated that high salinity positively influenced the mobility of all four elements, and species-specific translocation mechanisms may lead to their significant accretion in different tissues [74]. Moreover, both species efficiently took up Fe, Zn, Mn, and Cu, but none reached BAF values higher than 1. The BAF is widely used to characterize a plant as phytoremediator, and its value (higher than 1) is a crucial feature to ascertain a feasible hyperaccumulator [75]. In comparison with previous studies investigating the phytoremediation potential of halophytes [76–78], our results demonstrated that the investigated *Suaeda* species cannot be considered as metal accumulators, but they can be used for phytosequestration, especially for Zn and Cu.

FTIR is recognized as a non-destructive technique for exploring structural and chemical changes in plants under salinity stress conditions [79,80]. In this study, both species showed changes in the structural composition and functional groups of primary cellular metabolites, including lipids, proteins, and carbohydrates, detected as variable peaks in the FTIR spectra that are unique to bioactive metabolites found within both leaves and stem parts of plant species. Interestingly, the differential peaks at 1000–600 cm^{-1} revealed the significance of cell wall components in salinity tolerance. It can be argued that the differential responses of cellular metabolites may prevent the adverse impact of high salinity. Previous studies have revealed the application of FTIR-based metabolic analysis to infer salinity-induced responses in halophytes [14,81].

5. Conclusions

The findings of the present study suggested that a high salt content in soil threatens soil fertility and makes it highly susceptible to metal/metalloid corrosion. In the case of *Suaeda* plants, the presented results showed that both species considerably adjusted distinct physiological and biochemical attributes to tolerate high salinity via quantitative differences in their above-ground tissues. The high Na^+ level was accompanied by elevated K^+ and Ca^{2+} levels, which confirmed specific absorption and translocation mechanisms to avoid Na^+ toxicity. Proline acted as an efficient osmo-protective compound in both species to compensate for water loss and ionic toxicity, particularly in the stem. The presence of improved concentrations of soluble sugars and proteins implied a synergistic impact on osmotic adjustment in the leaves of both species. The observed accumulation of TPC was associated with robust antioxidant activity to reduce the oxidative damage caused by free radical ions. The FTIR profiles revealed differential cellular macromolecules that contribute to salinity tolerance. Due to the high capacity of Na^+ and Cl^- accumulation and considerable BAF values for metals, particularly Fe and Zn, *Suaeda* species (*S. nudiflora*, *S. fruticosa*) would be advisable for possible use in the phytoremediation of salt- and metal/metalloid-polluted soils.

Author Contributions: Conceptualization, A.J. and J.A.; Methodology, A.J., V.D.R. and J.A.; Validation, A.J. and J.A.; Formal Analysis, A.J., V.D.R., K.K.V., J.A. and T.M.; investigation, Resources, A.J. and J.A.; Data Curation, A.J. and J.A.; Writing—Original Draft Preparation, A.J. and J.A.; Writing—Review & Editing, A.J., V.D.R.; K.G., K.K.V. and J.A., Visualization, A.J. and J.A.; Supervision, J.A.; Project Administration. J.A.; Funding Acquisition, A.J., V.D.R. and J.A. All authors have read and agreed to the published version of the manuscript.

Funding: Not applicable.

Data Availability Statement: Not applicable.

Acknowledgments: We wish to acknowledge Prabhat Baroliya, MLSU, Udaipur, for providing the FTIR facilities. Abhishek Joshi acknowledges the support of UGC, New Delhi, for awarding the BSR meritorious fellowship [25-1/2014-15(BSR) 7-125/2007(BSR)]. V.D.R. and T.M. would like to acknowledge support from the laboratory of «Soil Health» of the Southern Federal University with the financial support of the Ministry of Science and Higher Education of the Russian Federation, agreement No. 075-15-2022-1122. K.G. acknowledge support by the Science Committee of RA, in the frames of the research project No 21AG-4C075.

Conflicts of Interest: The authors declare no conflict of interest.

References

1. FAO. Global Map of Salt-affected Soils (GSASmap). 2021. Available online: <https://www.fao.org/global-soil-partnership/gsasmap/en/> (accessed on 16 January 2022).
2. Hassani, A.; Azapagic, A.; Shokri, N. Global predictions of primary soil salinization under changing climate in the 21st century. *Nat. Commun.* **2021**, *12*, 6663. [[CrossRef](#)]
3. Shahid, S.A.; Zaman, M.; Heng, L. Soil salinity: Historical perspectives and a world overview of the problem. In *Guideline for Salinity Assessment, Mitigation and Adaptation Using Nuclear and Related Techniques*, 1st ed.; Zaman, M., Ed.; Springer: Cham, Switzerland, 2018; pp. 43–53.
4. Dagar, J.C. Salinity research in India: An overview. *Bull. Natl. Inst. Ecol.* **2005**, *15*, 69–80.
5. Mandal, A.K.; Reddy, G.O.; Ravisankar, T.; Yadav, R.K. Computerized database of salt-affected soils for coastal region of India. *J. Soil Salin. Water Qual.* **2018**, *10*, 1–13.
6. Flowers, T.J.; Colmer, T.D. Plant salt tolerance: Adaptations in halophytes. *Ann. Bot.* **2015**, *115*, 327–331. [[CrossRef](#)]
7. Mishra, A.; Tanna, B. Halophytes: Potential resources for salt stress tolerance genes and promoters. *Front. Plant Sci.* **2017**, *8*, 829. [[CrossRef](#)]
8. Zhao, C.; Zhang, H.; Song, C.; Zhu, J.K.; Shabala, S. Mechanisms of plant responses and adaptation to soil salinity. *Innovation* **2020**, *1*, 100017. [[CrossRef](#)]
9. Yadav, S.; Mishra, A. Ectopic expression of C4 photosynthetic pathway genes improves carbon assimilation and alleviate stress tolerance for future climate change. *Physiol. Mol. Biol. Plants.* **2020**, *26*, 195–209. [[CrossRef](#)]
10. Nikalje, G.C.; Srivastava, A.K.; Pandey, G.K.; Suprasanna, P. Halophytes in biosaline agriculture: Mechanism, utilization, and value addition. *Land Degrad. Dev.* **2018**, *29*, 1081–1095. [[CrossRef](#)]
11. Grigore, M.N.; Toma, C. Morphological and anatomical adaptations of halophytes: A review. In *Handbook of Halophytes: From Molecules to Ecosystems towards Biosaline Agriculture*, 1st ed.; Grigore, M.N., Ed.; Springer Nature: Cham, Switzerland, 2021; pp. 1079–1221.
12. Al Hassan, M.; Estrelles, E.; Soriano, P.; López-Gresa, M.P.; Bellés, J.M.; Boscaiu, M.; Vicente, O. Unravelling salt tolerance mechanisms in halophytes: A comparative study on four Mediterranean *Limonium* species with different geographic distribution patterns. *Front. Plant Sci.* **2017**, *8*, 1438. [[CrossRef](#)]
13. Podar, D.; Macalik, K.; Réti, K.O.; Martonos, I.; Török, E.; Carpa, R.; Székely, G. Morphological, physiological and biochemical aspects of salt tolerance of halophyte *Petrosimonia triandra* grown in natural habitat. *Physiol. Mol. Biol. Plants.* **2019**, *25*, 1335–1347. [[CrossRef](#)]
14. Joshi, A.; Kanthaliya, B.; Rajput, V.; Minkina, T.; Arora, J. Assessment of phytoremediation capacity of three halophytes: *Suaeda monoica*, *Tamarix indica* and *Cressa critica*. *Biologia Futr.* **2020**, *71*, 301–312. [[CrossRef](#)]
15. Joshi, A.; Kanthaliya, B.; Arora, J. Halophytic Plant Existence in Indian Salt Flats: Biodiversity, Biology, and Uses. In *Handbook of Halophytes: From Molecules to Ecosystems towards Biosaline Agriculture*; Grigore, M.N., Ed.; Springer Nature: Cham, Switzerland, 2020; pp. 1–22.
16. Joshi, A.; Kanthaliya, B.; Arora, J. Halophytes: The Nonconventional Crops as Source of Biofuel Production. In *Handbook of Halophytes: From Molecules to Ecosystems towards Biosaline Agriculture*, 1st ed.; Grigore, M.N., Ed.; Springer Nature: Cham, Switzerland, 2020; pp. 1–28.
17. Joshi, A.; Kanthaliya, B.; Arora, J. Halophytes of Thar Desert: Potential source of nutrition and feedstuff. *Int. J. Bioass.* **2018**, *8*, 5674–5683.

18. Sharma, V.; Joshi, A.; Ramawat, K.G.; Arora, J. Bioethanol production from halophytes of Thar Desert: A “green gold”. In *Environment at Crossroads: Challenges, Dynamics and Solutions*; Basu, S.K., Zandi, P., Chalaras, S.K., Eds.; Haghshenass Publishing: Guilan Prov, Iran, 2017; pp. 219–235.
19. Haque, M.I.; Siddiqui, S.A.; Jha, B.; Rathore, M.S. Interactive Effects of Abiotic Stress and Elevated CO₂ on Physio-Chemical and Photosynthetic Responses in *Suaeda* Species. *J. Plant Growth Regul.* **2021**, *41*, 2930–2948. [[CrossRef](#)]
20. Li, H.; Wang, H.; Wen, W.; Yang, G. The antioxidant system in *Suaeda salsa* under salt stress. *Plant Signal. Behav.* **2020**, *15*, 1771939. [[CrossRef](#)]
21. Joshi, A.; Kanthaliya, B.; Arora, J. Evaluation of growth and antioxidant activity in *Suaeda monoica* and *Suaeda nudiflora* callus cultures under sequential exposure to saline conditions. *Curr. Biotechnol.* **2019**, *8*, 42–52. [[CrossRef](#)]
22. Kumar, A.; Kumar, A.; Lata, C.; Kumar, S. Eco-Physiological responses of *Aeluropus lagopoides* (grass halophyte) and *Suaeda nudiflora* (non-grass halophyte) under individual and interactive sodic and salt stress. *S. Afr. J. Bot.* **2016**, *105*, 36–44. [[CrossRef](#)]
23. Hameed, A.; Hussain, T.; Gulzar, S.; Aziz, I.; Gul, B.; Khan, M.A. Salt tolerance of a cash crop halophyte *Suaeda fruticosa*: Biochemical responses to salt and exogenous chemical treatments. *Acta Physiol. Plant.* **2012**, *34*, 2331–2340. [[CrossRef](#)]
24. Song, J.; Wang, B. Using euhalophytes to understand salt tolerance and to develop saline agriculture: *Suaeda salsa* as a promising model. *Ann. Bot.* **2015**, *115*, 541–553. [[CrossRef](#)]
25. Ghanem, A.E.M.F.; Mohamed, E.; Kasem, A.M.; El-Ghamery, A.A. Differential salt tolerance strategies in three halophytes from the same ecological habitat: Augmentation of antioxidant enzymes and compounds. *Plants* **2021**, *10*, 1100. [[CrossRef](#)]
26. Ltaeif, H.B.; Sakhraoui, A.; González-Orenga, S.; LandaFaz, A.; Boscaiu, M.; Vicente, O.; Rouz, S. Responses to salinity in four *Plantago* species from Tunisia. *Plants* **2021**, *10*, 1392. [[CrossRef](#)]
27. Sinha, R. The Sambhar Lake: The Largest Saline Lake in Northwestern India. In *Landscapes and Landforms of India: World Geomorphological Landscapes*; Kale, V., Ed.; Springer: Dordrecht, The Netherlands, 2014; pp. 239–244.
28. Cherekar, M.N.; Pathak, A.P. Chemical assessment of Sambhar Soda Lake, a Ramsar site in India. *J. Water Chem. Technol.* **2016**, *38*, 244–247. [[CrossRef](#)]
29. USDA Handbook. *Diagnosis and Improvement of Saline and Alkali Soils*; Richards, L.A., Ed.; Oxford & IBH Publ. Co. Pvt. Ltd.: New Delhi, India, 1960; p. 60.
30. Olsen, S.R. *Estimation of Available Phosphorus in Soils by Extraction with Sodium Bicarbonate (No. 939)*; US Department of Agriculture: Washington, DC, USA, 1954.
31. Merwin, H.D.; Peech, M. Exchangeability of soil potassium in the sand, silt, and clay fractions as influenced by the nature of the complementary exchangeable cation 1. *Soil Sci. Soc. Am. J.* **1951**, *15*, 125–128. [[CrossRef](#)]
32. Prakash, L.; Prathapasenan, G. Effect of NaCl salinity and putrescine on shoot growth, tissue ion concentration and yield of rice (*Oryza sativa* L. var. GR-3). *J. Agron. Crop Sci.* **1988**, *160*, 325–334. [[CrossRef](#)]
33. Tüzen, M. Determination of heavy metals in soil, mushroom and plant samples by atomic absorption spectrometry. *Microchem. J.* **2003**, *74*, 289–297. [[CrossRef](#)]
34. Bates, C.J.; Waldren, R.P.; Teare, I.D. Rapid determination of free proline for water-stress studies. *Plant Soil.* **1973**, *39*, 205–207. [[CrossRef](#)]
35. Bradford, M.M. A rapid and sensitive method for the quantitation of microgram quantities of protein utilizing the principle of protein-dye binding. *Anal. Biochem.* **1976**, *72*, 248–254. [[CrossRef](#)]
36. Dubois, M.; Gilles, K.A.; Hamilton, J.K.; Rebers, P.T.; Smith, F. Colorimetric method for determination of sugars and related substances. *Anal. Chem.* **1956**, *28*, 350–356. [[CrossRef](#)]
37. Farkas, G.L.; Kiraly, Z. Role of phenolic compound in the physiology of plant diseases and disease resistance. *Phytopathol Zeitsch.* **1962**, *44*, 105–150. [[CrossRef](#)]
38. Hatano, T.; Kagawa, H.; Yasuhara, T.; Okuda, T. Two new flavonoids and other constituents in licorice root: Their relative astringency and radical scavenging effects. *Chem. Pharma. Bulletin.* **1988**, *36*, 2090–2097. [[CrossRef](#)]
39. Benzie, I.F.; Strain, J.J. The ferric reducing ability of plasma (FRAP) as a measure of “antioxidant power”: The FRAP assay. *Anal. Biochem.* **1996**, *239*, 70–76. [[CrossRef](#)]
40. Petelka, J.; Abraham, J.; Bockreis, A.; Deikumah, J.P.; Zerbe, S. Soil heavy metal (loid) pollution and phytoremediation potential of native plants on a former gold mine in Ghana. *Water Air Soil Pollu.* **2019**, *230*, 267. [[CrossRef](#)]
41. Hussain, S.; Shaukat, M.; Ashraf, M.; Zhu, C.; Jin, Q.; Zhang, J. Salinity stress in arid and semi-arid climates: Effects and management in field crops. In *Climate Change and Agriculture*; Intech Open: London, UK, 2019; p. 13. [[CrossRef](#)]
42. Kar, A. The Thar or the Great Indian Sand Desert. In *Landscapes and Landforms of India*; Kale, V.S., Ed.; Springer: Dordrecht, The Netherlands, 2014; pp. 79–90.
43. Chinnusamy, V.; Jagendorf, A.; Zhu, J.K. Understanding and improving salt tolerance in plants. *Crop Sci.* **2005**, *45*, 437–448. [[CrossRef](#)]
44. Ghazaryan, K.A.; Movsesyan, H.S.; Minkina, T.M.; Sushkova, S.N.; Rajput, V.D. The identification of phytoextraction potential of *Melilotus officinalis* and *Amaranthus retroflexus* growing on copper-and molybdenum-polluted soils. *Environ. Geochem. Health.* **2021**, *43*, 1327–1335. [[CrossRef](#)]
45. Kumar, V.; Sharma, A.; Kaur, P.; Sidhu, G.P.S.; Bali, A.S.; Bhardwaj, R.; Cerda, A. Pollution assessment of heavy metals in soils of India and ecological risk assessment: A state-of-the-art. *Chemosphere* **2019**, *216*, 449–462. [[CrossRef](#)]

46. Kumari, A.; Das, P.; Parida, A.K.; Agarwal, P.K. Proteomics, metabolomics, and ionomics perspectives of salinity tolerance in halophytes. *Front. Plant Sci.* **2015**, *6*, 537. [[CrossRef](#)]
47. Mangalassery, S.; Dayal, D.; Kumar, A.; Bhatt, K.; Nakar, R.; Kumar, A.; Misra, A.K. Pattern of salt accumulation and its impact on salinity tolerance in two halophyte grasses in extreme saline desert in India. *Indian J. Exp. Biol.* **2017**, *55*, 542–548.
48. Gil, R.; Bautista, I.; Boscaiu, M.; Lidón, A.; Wankhade, S.; Sánchez, H.; Vicente, O. Responses of five Mediterranean halophytes to seasonal changes in environmental conditions. *AoB Plants.* **2014**, *6*, plu049. [[CrossRef](#)] [[PubMed](#)]
49. Rahman, M.M.; Rahman, M.A.; Miah, M.G.; Saha, S.R.; Karim, M.A.; Mostofa, M.G. Mechanistic insight into salt tolerance of *Acacia auriculiformis*: The importance of ion selectivity, osmoprotection, tissue tolerance, and Na⁺ exclusion. *Front. Plant Sci.* **2017**, *8*, 155. [[CrossRef](#)]
50. Ahmed, H.A.I.; Shabala, L.; Shabala, S. Understanding the mechanistic basis of adaptation of perennial *Sarcocornia quinqueflora* species to soil salinity. *Physiol. Plant.* **2021**, *172*, 1997–2010. [[CrossRef](#)]
51. Kumar, A.; Mann, A.; Kumar, A.; Kumar, N.; Meena, B.L. Physiological response of diverse halophytes to high salinity through ionic accumulation and ROS scavenging. *Int. J. Phytoremediation* **2021**, *23*, 1041–1051. [[CrossRef](#)]
52. Chaudhary, D.R. Ion accumulation pattern of halophytes. In *Halophytes and Climate Change: Adaptive Mechanisms and Potential Uses*; Hasanuzzaman, M., Shabala, S., Fujita, M., Eds.; CAB International Publishing: Wallingford, UK, 2019; pp. 137–151.
53. Rahman, M.M.; Mostofa, M.G.; Keya, S.S.; Siddiqui, M.N.; Ansary, M.M.U.; Das, A.K.; Rahman, M.A.; Tran, L.S.P. Adaptive mechanisms of halophytes and their potential in improving salinity tolerance in plants. *Int. J. Mol. Sci.* **2021**, *22*, 10733. [[CrossRef](#)]
54. Ahmadi, F.; Mohammadkhani, N.; Servati, M. Halophytes play important role in phytoremediation of salt-affected soils in the bed of Urmia Lake, Iran. *Sci. Rep.* **2022**, *12*, 12223. [[CrossRef](#)] [[PubMed](#)]
55. Ravindran, K.C.; Venkatesan, K.; Balakrishnan, V.; Chellappan, K.P.; Balasubramanian, T. Restoration of saline land by halophytes for Indian soils. *Soil Biol. Biochem.* **2007**, *39*, 2661–2664. [[CrossRef](#)]
56. Devi, S.; Nandwal, A.S.; Angrish, R.; Arya, S.S.; Kumar, N.; Sharma, S.K. Phytoremediation potential of some halophytic species for soil salinity. *Int. J. Phytoremediation* **2016**, *18*, 693–696. [[CrossRef](#)] [[PubMed](#)]
57. Deinlein, U.; Stephan, A.B.; Horie, T.; Luo, W.; Xu, G.; Schroeder, J.I. Plant salt-tolerance mechanisms. *Trends Plant Sci.* **2014**, *19*, 371–379. [[CrossRef](#)] [[PubMed](#)]
58. Pardo-Domènech, L.L.; Tifrea, A.; Grigore, M.N.; Boscaiu, M.; Vicente, O. Proline and glycine betaine accumulation in two succulent halophytes under natural and experimental conditions. *Plant Biosyst.* **2016**, *150*, 904–915. [[CrossRef](#)]
59. Ghosh, U.K.; Islam, M.N.; Siddiqui, M.N.; Khan, M.A.R. Understanding the roles of osmolytes for acclimatizing plants to changing environment: A review of potential mechanism. *Plant Signal. Behav.* **2021**, *16*, 1913306. [[CrossRef](#)]
60. Slama, I.; Abdelly, C.; Bouchereau, A.; Flowers, T.; Savouré, A. Diversity, distribution and roles of osmoprotective compounds accumulated in halophytes under abiotic stress. *Ann. Bot.* **2015**, *115*, 433–447. [[CrossRef](#)]
61. Parida, A.K.; Panda, A.; Rangani, J. Metabolomics-guided elucidation of abiotic stress tolerance mechanisms in plants. In *Plant Metabolites and Regulation under Environmental Stress*; Ahmad, P., Ed.; Academic Press: Cambridge, MA, USA, 2018; pp. 89–131.
62. Saddhe, A.A.; Manuka, R.; Penna, S. Plant sugars: Homeostasis and transport under abiotic stress in plants. *Physiol. Plant.* **2021**, *171*, 739–755. [[CrossRef](#)]
63. Marco, P.; Carvajal, M.; del Carmen Martinez-Ballesta, M. Efficient leaf solute partitioning in *Salicornia fruticosa* allows growth under salinity. *Environ. Exper. Bot.* **2019**, *157*, 177–186. [[CrossRef](#)]
64. Mali, B.S.; Chitale, R.D. Comparison of accumulation of organic and inorganic osmolyte in *Trianthema portulacastrum* L. growing in saline and non-saline habitats. *Eco. Env. Cons.* **2020**, *26*, 155–158.
65. Akcin, A.; Yalcin, E. Effect of salinity stress on chlorophyll, carotenoid content, and proline in *Salicornia prostrata* Pall. and *Suaeda prostrata* Pall. subsp. *prostrata* (Amaranthaceae). *Braz. J. Bot.* **2016**, *39*, 101–106. [[CrossRef](#)]
66. Youssef, A.M. Salt tolerance mechanisms in some halophytes from Saudi Arabia and Egypt. *Res. J. Agric. Biol. Sci.* **2009**, *5*, 191–206.
67. Ibraheem, F.; Al-Zahrani, A.; Mosa, A. Physiological adaptation of three wild halophytic *Suaeda* species: Salt tolerance strategies and metal accumulation capacity. *Plants* **2022**, *11*, 537. [[CrossRef](#)]
68. Rajput, V.D.; Harish Singh, R.K.; Verma, K.K.; Sharma, L.; Quiroz-Figueroa, F.R.; Meena, M.; Mandzhieva, S. Recent developments in enzymatic antioxidant defence mechanism in plants with special reference to abiotic stress. *Biology* **2021**, *10*, 267. [[CrossRef](#)] [[PubMed](#)]
69. Waśkiewicz, A.; Muzolf-Panek, M.; Goliński, P. Phenolic content changes in plants under salt stress. In *Ecophysiology and responses of plants under Salt Stress*; Ahmad, P., Azooz, M., Prasad, M., Eds.; Springer: New York, NY, USA, 2013; pp. 283–314.
70. Benjamin, J.J.; Lucini, L.; Jothiramshekar, S.; Parida, A. Metabolomic insights into the mechanisms underlying tolerance to salinity in different halophytes. *Plant Physiol. Biochem.* **2019**, *135*, 528–545. [[CrossRef](#)]
71. Reginato, M.; Cenzano, A.M.; Arslan, I.; Furlán, A.; Varela, C.; Cavallin, V.; Luna, V. Na₂SO₄ and NaCl salts differentially modulate the antioxidant systems in the highly stress tolerant halophyte *Prosopis strombulifera*. *Plant Physiol. Biochem.* **2021**, *167*, 748–762. [[CrossRef](#)] [[PubMed](#)]
72. Lutts, S.; Lefèvre, I. How can we take advantage of halophyte properties to cope with heavy metal toxicity in salt-affected areas? *Ann. Bot.* **2015**, *115*, 509–528. [[CrossRef](#)] [[PubMed](#)]

73. Joshi, A.; Kanthaliya, B.; Meena, S.; Rajput, V.D.; Minkina, T.; Arora, J. Proteomic and Genomic Approaches to Study Plant Physiological Responses under Heavy Metal Stress. In *Heavy Metal Toxicity in Plants: Physiological and Molecular Adaptations*; Aftab, T., Hakeem, K.R., Eds.; CRC Press: Boca Raton, FL, USA, 2021; pp. 231–247.
74. Sánchez-Gavilán, I.; Rufo, L.; Rodríguez, N.; de la Fuente, V. On the elemental composition of the Mediterranean euhalophyte *Salicornia patula* Duval-Jouve (Chenopodiaceae) from saline habitats in Spain (Huelva, Toledo and Zamora). *Environ. Sci. Pollu. Res.* **2021**, *28*, 2719–2727. [[CrossRef](#)]
75. Rajput, V.; Minkina, T.; Semenov, I.; Klink, G.; Tarigholizadeh, S.; Sushkova, S. Phylogenetic analysis of hyperaccumulator plant species for heavy metals and polycyclic aromatic hydrocarbons. *Environ. Geochem. Health* **2021**, *43*, 1629–1654. [[CrossRef](#)]
76. Caparrós, P.G.; Ozturk, M.; Gul, A.; Batool, T.S.; Pirasteh-Anosheh, H.; Unal, B.T.; Altay, V.; Toderich, K.N. Halophytes have potential as heavy metal phytoremediators: A comprehensive review. *Environ. Exper. Bot.* **2022**, *193*, 104666. [[CrossRef](#)]
77. Alam, M.R.; Islam, R.; Tran, T.K.A.; Le Van, D.; Rahman, M.M.; Griffin, A.S.; Yu, R.M.K.; MacFarlane, G.R. Global patterns of accumulation and partitioning of metals in halophytic saltmarsh taxa: A phylogenetic comparative approach. *J. Hazard. Mater.* **2021**, *414*, 125515. [[CrossRef](#)]
78. Mousavi Kouhi, S.M.; Moudi, M. Assessment of phytoremediation potential of native plant species naturally growing in a heavy metal-polluted saline–sodic soil. *Environ. Sci. Pollu. Res.* **2020**, *27*, 10027–10038. [[CrossRef](#)] [[PubMed](#)]
79. Afifi, A.A.; Youssef, R.A.; Hussein, M.M. Fourier transform infrared spectrometry study on early stage of salt stress in *Jujube* plant. *Life Sci. J.* **2013**, *10*, 1973–1981.
80. Akyuz, S.; Akyuz, T.; Celik, O.; Atak, C. FTIR spectroscopy of protein isolates of salt-tolerant soybean mutants. *J. Appl. Spectroscopy.* **2018**, *84*, 1019–1023. [[CrossRef](#)]
81. Nikalje, G.C.; Kumar, J.; Nikam, T.D.; Suprasanna, P. FT-IR profiling reveals differential response of roots and leaves to salt stress in a halophyte *Sesuvium portulacastrum* (L.) L. *Biotechnol. Rep.* **2019**, *23*, e00352. [[CrossRef](#)] [[PubMed](#)]

Disclaimer/Publisher’s Note: The statements, opinions and data contained in all publications are solely those of the individual author(s) and contributor(s) and not of MDPI and/or the editor(s). MDPI and/or the editor(s) disclaim responsibility for any injury to people or property resulting from any ideas, methods, instructions or products referred to in the content.